Infrared Spectrum and Anharmonic Force Field of CH_2DBr

Agostino Baldacci, Paolo Stoppa,* Alessandro Baldan, and Santi Giorgianni

Dipartimento di Chimica Fisica, Università Ca′ Foscari di Venezia, Calle Larga S. Marta 2137, I-30123 Venezia, Italy

Alberto Gambi

Dipartimento di Scienze e Tecnologie Chimiche, Università degli Studi di Udine, Via Cotonificio 108, I-33100 Udine, Italy

Received: February 20, 2009; Revised Manuscript Received: April 8, 2009

The gas-phase infrared spectrum of monodeuteromethyl bromide, CH_2DBr, has been examined at medium resolution in the range 400−10000 cm^{-1}, leading to the identification of 70 vibrational transitions. The assignment of the absorptions in terms of fundamentals, overtones, combinations, and hot bands, assisted by quantum chemical calculations, is consistent all over the region investigated. The $^{79/81}Br$ isotopic splitting for the lowest fundamental ν_6 and the value for the $v_8 = 1$ level have been now precisely determined. Anharmonic resonances are very marginal for all fundamentals and the Coriolis interaction effects are clearly evident in the ν_4/ν_8 band system, in the ν_2 and ν_7 fundamentals. Spectroscopic parameters, obtained from the analysis of partially resolved rotational structure, have been derived in the symmetric tops limit approximation. High-quality ab initio calculations have been performed, and harmonic and anharmonic force fields have been predicted from coupled cluster CCSD(T) calculations employing the cc-pVTZ basis set. A good agreement between computed and experimental data, also including the C−H stretching overtones at 6000 and 9000 cm^{-1}, has been obtained.

1. Introduction

Methyl bromide, CH_3Br, released in the atmosphere from both natural and anthropogenic sources, is the most abundant long-lived bromocarbon in the troposphere.[1] This compound contributes ∼37% to all stratospheric bromine radicals,[2] which have been shown to be significantly involved in ozone depletion.[3] For this reason, CH_3Br is a molecule subjected to extensive spectroscopic and theoretical studies.[4,5]

Up to 1981 the infrared and microwave investigations of methyl bromide, including the fully and partially deuterated forms and ^{13}C isotopologue, have been critically collected and examined by Graner.[6] An extended assignment to the higher vibrational levels of CH_3Br and CD_3Br has been later performed in conjunction with a local and normal mode basis with addition of Fermi resonance.[7,8] As far as the theoretical investigations are concerned, harmonic and ab initio anharmonic force fields have been computed by Schneider and Thiel.[9−11] Recently, the molecular parameters (geometries, rotational constants, dipole moments) and vibrational harmonic wavenumbers with the integrated band intensities of bromomethanes have been obtained by density functional theory (B3LYP) and using ab initio second-order perturbation theory (MP2) and coupled cluster (CCSD(T)) calculations.[12] Absolute integrated intensities of the fundamental bands of the main and different deuterated species have been experimentally determined by Van Staten and Smit[13] showing that there is consistency with the early less accurate measurements performed only for the symmetric top species.[14−16]

Infrared spectra of the partially deuterated species of methyl halides (CH_2DX and CHD_2X with X = F, Cl, Br, I) were analyzed by Riter and Eggers,[17] and Raman data were obtained a long time ago.[18] The improved infrared techniques and the possibility of preparing pure samples of isotopic species make feasible a better understanding of the infrared absorption spectrum. Furthermore an extension of measurements in the overtone and combination regions allows the evaluation of a set of anharmonicity constants to be compared with those obtained from the anharmonic force field of methyl bromide.

In this work, the results obtained from the medium resolution infrared spectrum of CH_2DBr are reported. The pure sample has been prepared in the laboratory for spectroscopic investigations. All fundamentals and several overtone and combination bands show a partially resolved rovibrational structure which can be interpreted within the approximation limit of prolate symmetric tops. Concerning the fundamental frequencies, the results of ref 17 are confirmed; in addition the $v_8 = 1$ state value, early predicted from the assignment of uncertain combination bands, is now accurately obtained from the rovibrational interpretation of the complex ν_4/ν_8 band system.

The recent improvement of computer performances has enabled ab initio methods to include the anharmonic part of the molecular force field. The equilibrium structure and the harmonic force constants of CH_3Br (which apply also to all isotopologues) have been determined using high-level electronic-structure calculations, CCSD(T)/cc-pVTZ. Then cubic and semidiagonal quartic force constants for CH_2DBr have been conveniently calculated by numerical differentiation of analytical second derivatives obtained at the same level of theory after the isotopic mass substitution of one hydrogen with deuterium. These force constants have been used to estimate the anharmonic contribution to the fundamental vibrational wavenumbers as well as to assess and assist the whole assignment of the spectrum.

* Corresponding author, stoppa@unive.it.

10.1021/jp901577x CCC: $40.75
Published on Web 05/05/2009

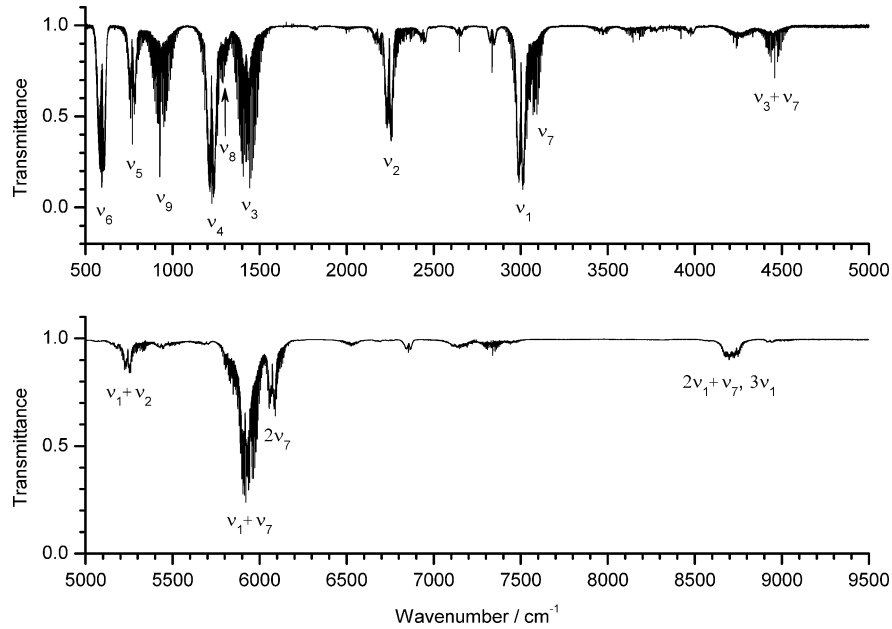

Figure 1. The gas-phase IR spectra of CH_2DBr: upper panel, resolution 0.2 cm^{-1}, path length 16 cm, pressure 108 mbar; lower panel, resolution 0.5 cm^{-1}, path length 16 cm, pressure ~1000 mbar. Only the stronger bands are labeled.

2. Experimental Details

2.1. Synthesis of the Sample. The sample of CH_2DBr was prepared by brominating methyl-d_1 alcohol, CH_2DOH (CDN Isotopes, 99.2% D atom) using potassium bromide, KBr (Sigma-Aldrich, 99%) and dilute H_2SO_4.[19] The reaction took place in an evacuated Pyrex tube, fitted with a HP Rotaflo stopcock and placed in a oven at 250 °C for 24 h. The product was separated from an excess of CH_2DOH by low temperature distillation under dynamic vacuum. No evidence of organic impurities was found by standard IR techniques.

2.2. Recording of the Spectra. The gas-phase infrared spectrum was recorded at room temperature in the range 400−10000 cm^{-1} at different resolving powers up to 0.2 cm^{-1}. The instrument was a Bruker Vertex 70 FTIR spectrometer equipped with a Ge/KBr beamsplitter, a Globar source, and a DTGS detector for the mid-IR and with a Si/CaF_2 beamsplitter, a tungsten lamp source, and a InGaAs detector for the near-IR region. A 16 cm path gas cell fitted with KBr windows was used with a sample pressure up to 1000 mbar.

2.3. Computational Details. The quantum mechanical calculations were carried out by means of the coupled cluster approach with single and double substitutions from the Hartree−Fock reference determinant with a perturbative treatment of triple excitations CCSD(T).[20]

In order to approach reasonable force field predictions,[21] it seems important to use spdf-type functions in the basis set for C/Br and spd-type function for H; hence all the computations were performed using the correlation-consistent polarized valence triple-ζ of Dunning,[22] cc-pVTZ. This basis set is described by [4s3p2d1f/3s2p1d] contraction of (10s5p2d1f/5s2p1d) primitive sets for C/H atoms[22] and by a [6s5p3d1f] contraction of the (20s13p9d1f) primitive set for the Br atom.[23]

Once the CCSD(T)/cc-pVTZ geometry optimization of the main isotopologue, CH_3Br, was determined, the harmonic force field at this equilibrium geometry was evaluated in the Cartesian coordinates representation employing the same level of theory. The CCSD(T)/cc-pVTZ cubic and quartic semidiagonal force constants (φ_{ijk}, φ_{ijkk}) were obtained in the reduced normal coordinates space with the use of a finite differences procedure,[10,24] involving displacements along normal coordinates (step size 0.05 amu$^{1/2}$ bohr) through analytical second derivatives at these displaced geometries. These calculations were performed with a local version of the Mainz−Austin−Budapest version of ACES II program package.[25] Spherical harmonic angular functions were used in all calculations, and all valence electrons were correlated (frozen core approximation).

3. Results and Discussion

The CH_2DBr molecule belongs to the C_s symmetry point group. The asymmetry parameter $\kappa = -0.997$, computed using the rotational constants derived at the equilibrium geometry, approaches the prolate symmetric rotor limit. The inertial *a* and *b* axes lie in the molecular symmetry plane, and the *c* axis is perpendicular to it. The nine fundamental modes are distributed in six of A′ and three of A″ species, all active in the infrared. The vibrations of A′ species are expected to appear as hybrid *a*-/*b*-type bands, where one component can prevail over the other, whereas those of A″ species originate *c*-type band envelopes. On the whole, the contours approach the parallel (*a*-type) and perpendicular (*b*- and *c*-type) bands of prolate symmetric tops. The difference of about 1 order of magnitude of *A* compared to *B* and *C* rotational constants produces *a*-type bands spanning in a narrower wavenumber range (~60 cm^{-1}) with respect to the *b*-/*c*-type bands (~140 cm^{-1}). Thus for hybrid bands the rovibrational structure of the ^qP and ^qR multiplets can be easily discriminated from those ascribed to the $^{p,r}Q$ multiplets. In the absence of strong resonances and excluding the sublevels with $K_a = 1$ and to a lesser extent those with $K_a = 2$ for the asymmetry splitting, the *b*- and *c*-type bands manifest a series of regularly spaced $^{p,r}Q$ subbranches. Consequently, their assignment allows a rough determination of the rotational constants. Most of the line frequencies were measured from spectra recorded at 0.2 cm^{-1} resolution. In these conditions neither the *K* structure of the $^qP(J)$, $^qR(J)$ parallel clusters nor the *J* structure of the perpendicular ^pQ_K and ^rQ_K subbranches can be resolved. The $^{79/81}$Br isotopic shift was detected only for a few bands and in particular for those exhibiting a predominant *a*-type structure and involving the ν_6 vibration which is associated to the C−Br stretching of the molecule.

TABLE 1: Geometrical Parameters[a] and Internal and C_s Point Group Symmetry Coordinates[b] of CH_2DBr

C−H = 1.0851 Å; C−Br = 1.9474 Å; H−C−H = 110.96°; H−C−Br = 107.94°	
r_i = C−H$_i$ (i = 1, 2); R = C−Br; r = C−D; α = H−C−H; α$_i$ = H$_i$−C−D (i =1, 2); β_i = H$_i$−C−Br (i = 1, 2)	
A′	$S_1 = (1/2^{1/2})(r_1 + r_2)$
	S_2 (4a) = r
	$S_3 = R$
	$S_4 = \alpha$
	S_5 (5a) = $(1/2^{1/2})(\alpha_1 + \alpha_2)$
	S_6 (6a) = $(1/2^{1/2})(\beta_1 + \beta_2)$
A″	S_7 (4b) = $(1/2^{1/2})(r_1 - r_2)$
	S_8 (5b) = $(1/2^{1/2})(\alpha_1 - \alpha_2)$
	S_9 (6b) = $(1/2^{1/2})(\beta_1 - \beta_2)$

[a] Equilibrium geometry from CCSD(T)/cc-pVTZ calculations. [b] The corresponding labels in the C_{3v} point group symmetry coordinates of CH_3Br are indicated in parentheses.

The infrared survey gas-phase spectrum of CH_2DBr, showing all fundamental bands, is reported in Figure 1. In addition a number of complex regions corresponding to the strongest overtones and combination bands are also indicated.

3.1. Equilibrium Geometry. As a large number of computational studies has shown, the coupled-cluster singles and doubles approach[26] augmented by a perturbative treatment of triple excitations CCSD(T)[20] yields near quantitative accuracy in many cases, provided that sufficiently large basis sets are used.[27]

For geometries, it has been found that CCSD(T)/cc-pVTZ calculations typically yield results with a residual error of 0.005 Å for bond lengths and 0.2° for bond angles[28]when compared to reliable $r_e$structures. On this basis the geometry optimization of CH_3Br was carried out at the CCSD(T)/cc-pVTZ level of theory using analytic gradients. The geometry calculations converged in such a manner that all distances are precise to at least 0.0001 Å. The three geometrical parameters which define the structure of CH_3Br, i.e., the C−H and C−Br bonds and H−C−H angle evaluated at the CCSD(T)/cc-pVTZ level of theory are given in the upper part of Table 1. For the sake of completeness, the H−C−Br angle is included. The chemically intuitive internal coordinates of CH_2DBr and the symmetry coordinates, obtained from the internal ones applying the C_s symmetry point group rules, are also reported in Table 1. The corresponding S_{na} and S_{nb} (with n = 4, 5, and 6) symmetry coordinates of the degenerate E symmetry species in the C_{3v} point group of CH_3Br[29] are indicated in the same table.

3.2. Harmonic and Anharmonic Force Fields. The CCSD-(T)/cc-pVTZ harmonic force field, obtained in a Cartesian coordinate representation at the equilibrium geometry optimized at the same level of theory, was evaluated for the main isotopic species, CH_3Br. In order to obtain a complete description of the molecular motions involved in the normal modes of CH_2DBr, a normal coordinate analysis was carried out. The ab initio force constants were used in a mass weighted Cartesian coordinates calculation to produce the theoretical vibrational frequencies and to determine the total energy distribution (TED).[30]

The predicted fundamental harmonic wavenumbers for CH_2DBr are given in Table 2. The TED % of each normal mode, expressed in terms of the symmetry coordinates of Table 1, is also indicated. The last two columns of Table 2 report, respectively, the theoretical and experimental integrated infrared band intensities of each fundamental. The computed band intensities were obtained from the formula

$$A_i = 42.25472\left|\frac{\partial \mu}{\partial Q_i}\right|^2 \quad (1)$$

where A_i is in km/mol, and $\partial\mu/\partial Q_i$ in D/(Å amu$^{1/2}$) are the dipole moment derivatives evaluated analytically at CCSD(T)/cc-pVTZ level of theory. There is a general good agreement between observed and computed intensity values with exclusion of the ω_4 and ω_8 modes discussed in the next section.

The cubic and quartic semidiagonal force constants were predicted in the normal coordinates space with the use of a finite difference procedure, as outlined in section 2.3, through the calculation of analytical second derivatives at these displaced geometries. Since the normal-coordinates force constants are mass-dependent, the displacements along the normal coordinates refer to the $CH_2D^{79}Br$ molecule and appropriate eigenvalues and eigenvectors of the mass-weighted Cartesian force constants matrix were employed.[10] Applying the formulas based on second-order perturbation theory,[31] which include cubic (φ_{ijk}) and quartic (φ_{iiii} and φ_{iijj}) normal coordinates force constants, the anharmonic spectroscopic parameters could be determined.

3.3. The Fundamental Bands. The ν_3, ν_5, ν_6, and ν_9 fundamentals exhibit clear contours typical of single bands while ν_1 overlaps ν_7, ν_4 almost completely obscures ν_8, and ν_2 is surrounded on both wavenumber sides by the structure of combination bands. Among the vibrations of A′ symmetry species, ν_1, ν_2, ν_4, and ν_5 show predominant a-type character with a series of regularly spaced Q multiplets in the P and R branches; ν_3 displays a predominant b-type contour while ν_6 manifests a pure a-type envelope. For this fundamental an easily discernible $^{79/81}$Br isotopic shift is apparent in the details illustrated in Figure 2.

The characteristics of the fundamental bands are collected in Table 3 together with those of several other bands which are discussed in the next section. There is a general agreement with the results of ref 17 with the exception of ν_8, whose previous frequency value could not be directly measured. According to the new value of ν_8, blue shifted about 12 cm^{-1} compared to the previous one,[17] the absolute intensities of the overlapped ν_4/ν_8 band system of Van Staten and Smit[13] are to be revised, thus aligning much better with the predicted ones of the same authors and with our calculations (see Table 2).

The improved accuracy of the band origins and the additional information obtained in the present study mainly derive from the assigned structure for all the fundamental bands with the exception of ν_6, and the treatment of the observed data through polynomial fits.

3.4. Overtones and Combination Bands. A significant number of overtones and combinations were identified in the spectra. The vibrational frequencies are collected in Table 3 in order of increasing wavenumber values. First overtones and two quanta combinations were assigned using frequency predictions based on additivity of the fundamentals. The ab initio calculated intensities were also considered to discriminate between bands expected in the same spectral range. This is the case for the 4200−4500 cm^{-1} region which shows irregular contours due to overlapping of seven absorption bands and strong perturbation effects.

The spectral region of the C−H stretching first overtones is reproduced in Figure 3. Here the hybrid character of $2\nu_7$ is evident whereas $2\nu_1$, heavily overlapped by $\nu_1 + \nu_7$, shows a predominant a-type character. The additional band, observed

TABLE 2: Harmonic Wavenumbers ω_i, Total Energy Distribution (TED %), and Integrated Infrared Band Intensities of CH_2DBr

		calculated[a]			
symmetry species	mode	TED %[c]	wavenumbers (cm^{-1})	intensities (km/mol)	experimental intensities[b] (km/mol)
A′	ω_1	S_1 (100)	3128	11.5	11.737 ± 0.326[d]
	ω_2	S_2 (99)	2313	5.8	4.866 ± 0.053
	ω_3	S_4 (78) + S_5 (17)	1463	7.0	8.603 ± 0.075
	ω_4	S_5 (66) + S_6 (32)	1252	18.5	12.759 ± 0.290[e]
	ω_5	S_6 (55) + S_5 (21) + S_4 (19)	779	3.9	3.544 ± 0.037
	ω_6	S_3 (98)	605[f]	7.2	9.010 ± 0.068
A″	ω_7	S_7 (100)	3195	2.5	2.934 ± 0.326[d]
	ω_8	S_8 (87) + S_9 (13)	1284	1.5	4.962 ± 0.290[e]
	ω_9	S_9 (87) + S_8 (13)	942	4.1	4.343 ± 0.070

[a] CCSD(T)/cc-pVTZ level of theory. [b] Reference 13. [c] Terms ≥10%; symmetry coordinates defined in Table 1. [d] Overlapping bands ν_1 and ν_7. [e] Overlapping bands ν_4 and ν_8. [f] 604 cm^{-1} for the $CH_2D^{81}Br$ isotopologue.

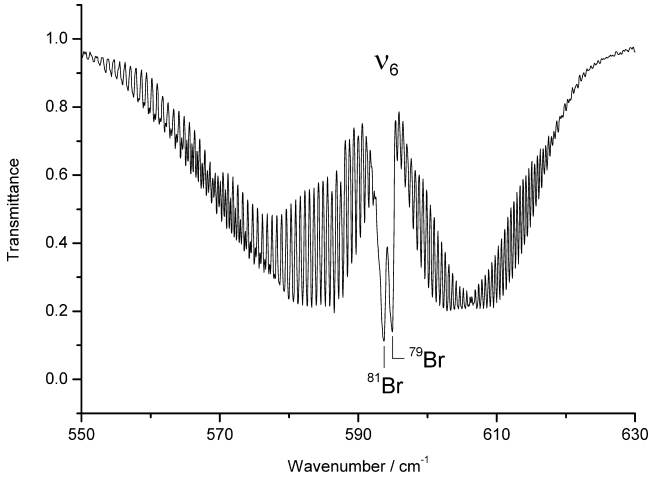

Figure 2. The FTIR spectral region of the ν_6 fundamental of CH_2DBr (resolution 0.2 cm^{-1}, path length 16 cm, pressure 108 mbar) showing the *a*-type band envelope and the $^{79/81}Br$ isotopic splitting.

in the lower wavenumber side, was attributed to $2\nu_3 + \nu_7$. The possible alternative assignment $2\nu_2 + \nu_3$ was ruled out on the basis of different symmetry species and the consequently expected different band contour. In total 29 of the 45 expected bands referring to first overtones and two quanta combinations were identified. Several of the remaining unassigned absorptions are predicted to have a very low intensity, and some of them are buried under stronger absorptions. The vibrational values were subsequently taken into account as a useful guide for the identification of the even weaker bands with higher number of quanta. In addition two hot bands, implying $v_6 = 1$ as lower state, could be assigned with confidence.

3.5. Rovibrational Analysis. All fundamentals and many other bands manifest the peculiar structure of molecules with relatively large rotational constants. A typical characteristic of A′ mode with predominant *a*-type component is given by the ν_6 band illustrated in Figure 2 where the $^qP, R$) multiplets are observed in sequence with a separation governed by the term $2\bar{B} = (B + C) = 0.58$ cm^{-1}. The unstructured *Q*-branch degrading to the lower wavenumbers indicates that the value $(\alpha^A - \alpha^B) = [(A_0 - A') - (B_0 - B')]$ is negative and very small. The *Q*-branches of ν_1 and ν_2 degrade in the same way as ν_6 whereas for ν_3, ν_4, and ν_5 the degradation occurs in the opposite direction. The *Q*-branches of ν_1 and ν_2 display partially resolved ^qQ_K subbranches covering a spectral range of about 5 cm^{-1}. The inherent qualitative observations are confirmed by the calculated rotational constants predicted from the theoretical results.

Of the three fundamentals of A″ symmetry the structure of ν_9 and that of the partially masked ν_7 is well-defined whereas ν_8, the weakest fundamental strongly overlapped by the *a*-type component of ν_4, shows a limited and irregular series of $^{p,r}Q$ peaks.

None of the fundamental vibrations is affected by significant anharmonic vibrational resonances; however perturbation effects due to strong Coriolis interactions were detected in the spectral regions of ν_4/ν_8, ν_2, and ν_7. In proximity of the levels crossing, the observed clusters appear broader and shifted compared to the unperturbed predicted values. In detail these effects were detected in the spectrum for the sublevels with $K_a = 4, 5$ of ν_4, $K_a = 3, 4$ of ν_3, and $K_a = 9, 10$ of ν_2; anomalies were also observed for $K_a = 3, 4, 5$ of ν_7 where the related Q_K multiplets, clearly seen in the *R*-branch, originate split lines of different strength.

The interpretation of the resolved structure was first devoted to the *b*- and *c*-type components of the simpler bands. The *K* numbering of the $^{p,r}Q_K$ subbranches of the hybrid bands was easily found by taking into account the central *Q*-branch whereas for *c*-type bands the effect of asymmetry splitting for the lower K_a sublevels was mandatory for the line assignment. An example is reported in Figure 4 where details of the ν_9 spectral region are reproduced.

A set of ground-state combinations-differences was calculated from the structure of the *b*- and *c*-type bands. Subsequently the obtained term values were used as a guide for the assignment of the complex spectral regions in particular in the ν_4/ν_8 band system and in the more congested and complicated regions of the overtone and combination bands.

The following simplified equation, usually exploited for $^{p,r}Q_K$ features in symmetric tops, was adopted for the evaluation of the spectroscopic parameters

$$\tilde{\nu}^{P,R} = \tilde{\nu}_0 + (A' - \bar{B}') \mp 2(A' - \bar{B}')K + [(A' - \bar{B}') - (A_0 - \bar{B}_0)]K^2 \pm 4D'_K K^3 \quad (2)$$

where the upper and lower signs apply for the *P*- and *R*-branchs, respectively.

The results, obtained for the fundamental vibrations using the above expression, are summarized in the upper part of Table 4; only for ν_4 the cubic term in *K* was neglected since no physical meaning of D'_K was obtained. Within the approximation of this analysis most of the determined spectroscopic parameters are consistent with the predicted values. The average value of $(A_0 - \bar{B}_0)$ was determined with the exclusion of ν_4 since the corresponding value was much lower than all the others. For comparison the calculated value is reported in the footnote of

TABLE 3: Summary of the Assigned Bands (cm^{-1}) Obtained from the Gas-Phase Infrared Spectrum of CH_2DBr

band	envelope	rel intens[a]	wavenumber[b]
ν_6	A	s	595.0(2)/593.8(2)[c]
$2\nu_6 - \nu_6$			587.8(3)/586.6(3)[c]
ν_5	A/B	m	768.76(2)[d]
ν_9	C	m	930.28(1)[d]
ν_4	A/B	s	1225.21(5)[d]
ν_8	C	w	1252.55(3)[d]
ν_3	A/B	s	1424.94(1)[d]
$\nu_4 + \nu_6$	A	vw	1817.8(3)/1816.6(3)[c]
$2\nu_9$	B	vvw	1858.51(15)[d]
$\nu_4 + \nu_5$	B	vw	1989.65(10)[d]
$\nu_5 + \nu_8$	C	vw	2016.70(7)[d]
$\nu_8 + \nu_9$	A/B	w	2176.2(3)
ν_2	A/B	m	2243.80(1)[d]
$\nu_3 + \nu_9$	C	w	2346.86(2)[d]
$2\nu_4$	A	w	2442(1)
$\nu_4 + \nu_8$	C	vw	2470.0(3)
$2\nu_8$	A	vvw	2499(1)
$\nu_3 + \nu_4$	A/B	w	2646.91(3)[d]
$\nu_3 + \nu_5 + \nu_6$	A	vvw	2779.6(3)/2778.2(3)[c]
$2\nu_3$	A/B	w	2835.3(3)
$2\nu_3 + \nu_6 - \nu_6$			2833.8(4)
ν_1	A/B	s	3001.04(1)[d]
ν_7	C	m	3052.96(2)[d]
$2\nu_4 + \nu_5$	A	vvw	3201(2)
$\nu_2 + \nu_4$	A/B	w	3464.47(4)[d]
$\nu_2 + \nu_8$	C	vvw	3486(2)
$\nu_1 + \nu_6$	A/B	vvw	3595(1)
$\nu_2 + \nu_3$	B	w	3664.75[d]
$\nu_1 + \nu_5$	A/B	w	3768.63(3)[d]
$\nu_5 + \nu_7$	C	vw	3821.30(15)[d]
$\nu_1 + \nu_9$	C	w	3923.45(4)[d]
$\nu_7 + \nu_9$	A	w	3977.2(5)
$2\nu_3 + \nu_4$	A/B	vvw	4059(2)
$\nu_1 + \nu_4$	A/B	vw	4222(1)
$\nu_1 + \nu_8$	C	vw	4241(1)
$2\nu_2$	B	vw	4437(2)
$\nu_3 + \nu_7$	C	m	4456.49(2)[d]
$\nu_1 + \nu_5 + \nu_9$	C	vvw	4693.66(11)[d]
$\nu_5 + \nu_7 + \nu_9$	A/B	vw	4747.04(5)[d]
$\nu_1 + 2\nu_9$	A/B	vw	4844.6(3)
$\nu_7 + 2\nu_9$	C	vw	4897.85(7)[d]
$\nu_2 + 2\nu_3$	A/B	vvw	5071.5(3)
$\nu_1 + \nu_8 + \nu_9$	A/B	vvw	5154.95(4)[d]
$\nu_1 + \nu_2$	A/B	w	5241.79(4)[d]
$\nu_2 + \nu_7$	C	vvw	5295.31(6)[d]
$\nu_1 + 2\nu_4$	A	vvw	5434(1)
$\nu_4 + \nu_7 + \nu_8$	A/B	vvw	5503(1)
$\nu_7 + 2\nu_8$	C	vvw	5530(1)
$\nu_1 + \nu_3 + \nu_8$	C	vvw	5651(1)
$\nu_3 + \nu_7 + \nu_8$	A/B	vw	5695.8(3)
$2\nu_3 + \nu_7$	C	vw	5843.87(7)[d]
$2\nu_1$	B	vw	5915.18(11)[d]
$\nu_1 + \nu_7$	C	w	5939.21(3)[d]
$2\nu_7$	A/B	vw	6072.21(4)[d]
$\nu_2 + \nu_7 + \nu_8$	B	vvw	6515.20(5)[d]
$3\nu_2$	A	vvw	6553(1)
$2\nu_1 + \nu_5$	A	vvw	6679(1)
$\nu_1 + \nu_5 + \nu_7$	C	vvw	6694.49(13)[d]
$\nu_5 + 2\nu_7$	A	vvw	6840(1)
$\nu_1 + \nu_7 + \nu_9$	A	vvw	6856(1)
$2\nu_7 + \nu_9$	C	vvw	6981.41(10)[d]
$2\nu_1 + \nu_4$	A/B	vvw	7133(2)
$\nu_1 + \nu_7 + \nu_8$	B	vvw	7174.63(9)[d]
$\nu_1 + \nu_3 + \nu_7$	C	vvw	7335.04(5)[d]
$\nu_3 + 2\nu_7$	A/B	vvw	7459.01(6)[d]
$\nu_2 + 2\nu_7$	A	vvw	8316(1)
$2\nu_1 + \nu_7$	C	vvw	8702.02(10)[d]
$3\nu_1$	A/B	vvw	8738.44(7)[d]
$\nu_1 + 2\nu_7$	A/B	vvw	8931.49(7)[d]
$3\nu_7$	C	vvw	9012.92(6)[d]

[a] Abbreviations used are as follows: s = strong, m = medium, w = weak, vw = very weak, vvw = very very weak. [b] The experimental error in parentheses is on the last significant digits. [c] The values rely with the $^{79/81}Br$ isotopologues. [d] Value obtained from the fit of $^{p,r}Q_K(J)$-manifolds of *b*- and *c*-type bands (see text).

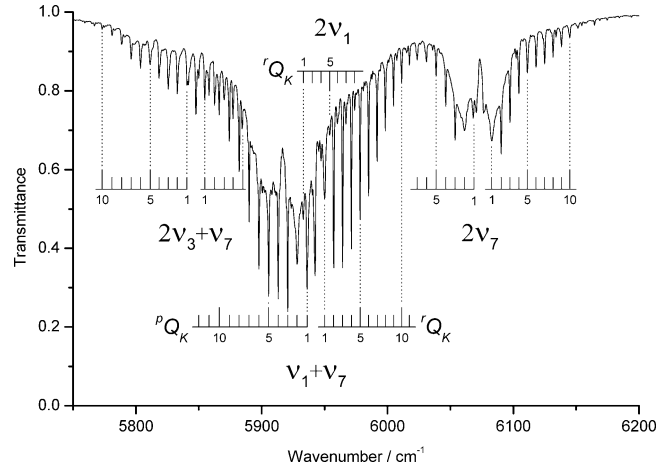

Figure 3. The FTIR spectral region of the CH_2 stretching overtones and combination bands of CH_2DBr (resolution 0.5 cm^{-1}, path length 16 cm, pressure ~1000 mbar).

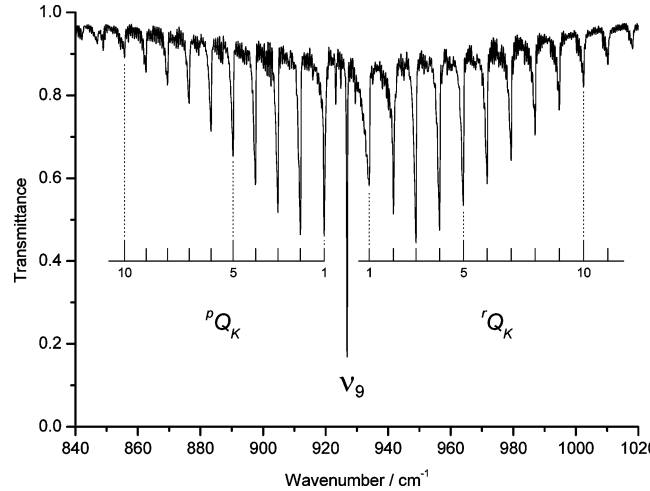

Figure 4. The FTIR spectral region of the ν_9 CH_2 rocking fundamental (*c*-type) of CH_2DBr (resolution 0.2 cm^{-1}, path length 16 cm, pressure 108 mbar).

the same table. The D'_K centrifugal distortion constant values are similar to the calculated ground-state value ($D_K = 0.55 \times 10^{-4}$ cm^{-1}) with exclusion of ν_7 whose value was obtained from a fit of few ^pQ multiplets. In the lower section of Table 4 the results of the structured bands up to three quanta are also included. Using the $(\alpha^A - \alpha^{\bar{B}})$values of the fundamental levels and applying the additivity method, a satisfactory consistency was obtained for all the bands thus giving further support to the assignment.

3.6. The Anharmonicity Constants. For an asymmetric top, the vibrational energy levels are given by[32]

$$G(v) = \sum \omega_i\left(\mathrm{v}_i + \frac{1}{2}\right) + \sum_{i \le j} x_{ij}\left(\mathrm{v}_i + \frac{1}{2}\right)\left(\mathrm{v}_j + \frac{1}{2}\right) \tag{3}$$

So the fundamental frequencies ν_i are given by

$$\nu_i = \omega_i + 2x_{ii} + \frac{1}{2}\sum_{j \neq i} x_{ij} \tag{4}$$

with $x_{ij} = x_{ji}$.

From a number of selected bands given in Table 3, the anharmonicity constants were obtained by applying these expressions.

TABLE 4: Spectroscopic Parameters (cm^{-1}) from *b*- and *c*-Type Bands of CH_2DBr[a]

band	ν_0	$(A' - \bar{B}')$	$(\alpha^A - \alpha^{\bar{B}}) \times 10^2$	$D'_K \times 10^4$	$(A_0 - \bar{B}_0)$	σ^b	no. of data
ν_1	3001.044(10)	3.6503(10)	2.80(2)	0.56(6)	3.6783(10)	0.0006	19
ν_2	2243.802(13)	3.6429(14)	3.58(3)	0.48(11)	3.6787(14)	0.0008	16
ν_3	1424.944(15)	3.6752(15)	0.07(2)	0.32(9)	3.6759(15)	0.0014	18
ν_4	1225.21(5)	3.6793(18)	−0.98(6)		3.6695(19)	0.0047	10
ν_5	768.76(2)	3.685(2)	−0.69(4)	0.7(2)	3.678(2)	0.0009	12
ν_7	3052.96(2)	3.660(2)	1.51(16)	1.7(3)	3.675(3)	0.0006	10
ν_8	1252.55(3)	3.627(2)	5.25(3)	0.63(9)	3.680(2)	0.0011	11
ν_9	930.281(8)	3.7095(9)	−2.46(2)	0.94(8)	3.6849(9)	0.0003	15
					3.679(5)[c] (average)		
$2\nu_9$	1858.51(15)	3.744(16)	−4(2)		3.70(3)	0.028	5
$\nu_4 + \nu_5$	1989.65(10)	3.700(5)	−2.0(2)		3.680(6)	0.036	12
$\nu_5 + \nu_8$	2016.70(7)	3.629(3)	4.34(13)		3.672(3)	0.013	13
$\nu_3 + \nu_9$	2346.86(2)	3.7033(18)	−2.29(3)	0.41(11)	3.6804 (18)	0.002	18
$\nu_3 + \nu_4$	2646.91(3)	3.684(3)	−0.44(4)	0.46(15)	3.679(3)	0.006	18
$\nu_2 + \nu_4$	3464.47(4)	3.657(4)	2.66(6)	0.6(2)	3.683(4)	0.007	17
$\nu_2 + \nu_3$	3664.75(4)	3.6335(17)	3.95(7)		3.6730(19)	0.010	17
$\nu_1 + \nu_5$	3768.63(3)	3.656(3)	2.06(14)		3.677(3)	0.005	9
$\nu_5 + \nu_7$	3821.30(15)	3.65(2)	3(2)		3.68(3)	0.050	7
$\nu_1 + \nu_9$	3923.45(4)	3.681(4)	−0.32(12)		3.677(4)	0.009	14
$\nu_3 + \nu_7$	4456.49(2)	3.6691(14)	1.239(17)	0.72(6)	3.6815(14)	0.002	23
$\nu_1 + \nu_5 + \nu_9$	4693.66(11)	3.689(6)	−1.4(5)		3.676(8)	0.026	7
$\nu_5 + \nu_7 + \nu_9$	4747.04(5)	3.680(3)	−1.59(18)		3.664(4)	0.011	13
$\nu_7 + 2\nu_9$	4897.85(7)	3.715(5)	−3.1(3))		3.684(6)	0.018	11
$\nu_1 + \nu_2$	5241.79(4)	3.609(2)	6.27(8)		3.671(2)	0.007	14
$\nu_2 + \nu_7$	5295.31(6)	3.621(7)	5.3(2)		3.674(8)	0.016	11
$2\nu_3 + \nu_7$	5843.87(7)	3.683(6)	−0.4(3)		3.679(7)	0.018	10
$2\nu_1$	5915.18(11)	3.626(10)	4.8(4)		3.674(10)	0.033	7
$\nu_1 + \nu_7$	5939.21(3)	3.634(3)	4.15(4)	0.47(14)	3.676(3)	0.007	23
$2\nu_7$	6072.21(4)	3.633(3)	3.73(12)		3.670(3)	0.010	15
$\nu_2 + \nu_7 + \nu_8$	6515.20(5)	3.588(3)	9.11(14)		3.679(3)	0.014	15
$\nu_1 + \nu_5 + \nu_7$	6694.49(13)	3.656(11)	3.2(6)		3.689(13)	0.042	8
$2\nu_7 + \nu_9$	6981.41(10)	3.679(7)	0.8(4)		3.687(8)	0.023	8
$\nu_1 + \nu_7 + \nu_8$	7174.63(9)	3.571(8)	10.4(4)		3.675(9)	0.019	6
$\nu_1 + \nu_3 + \nu_7$	7335.04(5)	3.654(7)	3.06(12)	1.2(6)	3.684(7)	0.017	17
$\nu_3 + 2\nu_7$	7459.01(6)	3.652(4)	1.95(25)		3.671(5)	0.014	12
$2\nu_1 + \nu_7$	8702.02(10)	3.641(8)	2.0(3)		3.661(8)	0.045	12
$3\nu_1$	8738.44(7)	3.613(5)	2.5(4)		3.638(6)	0.013	9
$\nu_1 + 2\nu_7$	8931.49(7)	3.593(4)	6.8(2)		3.661(5)	0.016	11
$3\nu_7$	9012.92(6)	3.623(4)	4.5(2)		3.668(4)	0.011	10

[a] The uncertainties given in parentheses are 1 standard deviation of the last significant digits. [b] Standard deviation (cm^{-1}). [c] The average does not include the $(A_0 - \bar{B}_0)$ value of ν_4; calculated theoretical value $(A_0 - \bar{B}_0) = 3.674\ cm^{-1}$.

TABLE 5: Anharmonicity Constants x_{ij} (cm^{-1}) of $CH_2D^{79}Br$[a]

i	*j* = 1	*j* = 2	*j* = 3	*j* = 4	*j* = 5	*j* = 6	*j* = 7	*j* = 8	*j* = 9
1	−43.4 (−28.4)	−3.0 (−2.5)	−12[b] (−8.1)	−4 (−3.6)	−1.2 (−0.9)	−1 (+1.4)	−114.8 (−117.6)	−12 (−10.8)	−7.9 (−7.0)
2		−25 (−32.0)	−4.0 (−3.4)	−4.5 (−3.5)	− (−3.3)	− (0.0)	−1.4 (−0.2)	−10 (−9.3)	− (+2.3)
3			−7.3 (−6.7)	−3.2 (−2.5)	−[c] (−2.2)	−0.7 (−0.6)	−21.4 (−22.1)	−3[b] (−2.8)	−8.4 (−7.8)
4				−4 (−4.4)	−4.3 (−3.6)	−2.4 (−1.6)	−9[b] (−10.2)	−7.8 (−6.2)	− (−0.1)
5					− (−1.4)	−[c] (−4.5)	−0.4 (−1.3)	−4.6 (−4.4)	+2.7[b] (+3.3)
6						−3.6 (−3.5)	− (+2.2)	− (−1.1)	− (−6.2)
7							−16.9 (−33.0)	−11[b] (−12.2)	−6.0 (−6.4)
8								−3 (−1.9)	−6.6 (−6.7)
9									−1.0 (−0.6)

[a] The calculated values given in parentheses are from the CCSD(T)/cc-pVTZ anharmonic force field. [b] From vibrational levels with three quantum numbers. [c] $x_{35} + x_{56} = -8.4\ (-6.7)$.

The results, summarized in Table 5, account for 35 of the 45 determinable constants. The reported values were obtained by excluding any vibrational perturbation; this is the reason of the noticeable discrepancies between the empirical and calculated values of x_{11} and x_{77} determined by using the $2\nu_1$ and $2\nu_7$ overtones interacting by Darling−Dennison resonance. In the same way the discrepancy of the x_{22} can be readily justified by the undetected anharmonic resonance between the $2\nu_2$ and $\nu_1 + \nu_3$ levels predicted to be very close in energy. Using the fundamental band origins, 31 constants were obtained from first overtones, combinations with two quanta and hot bands, and four constants by taking into account bands with three quanta. The values of x_{35} and x_{56} could not be discriminated; hence they are given as a summation term. In the same table the calculated anharmonicity constants x_{ij} are given in parentheses. They were obtained from the theoretical cubic and quartic normal coordinates force constants by applying the formulas based on second-order perturbation theory.[31] These constants were then employed

TABLE 6: Vibrational Frequencies (cm^{-1}) of the Fundamental Bands of $CH_2D^{79}Br$

symmetry species	mode	approximate description	calculated[a]	(obsd − calcd)[b]
A′	ν_1	CH_2 sym. stretch	2997	4
	ν_2	CD stretch	2239	5
	ν_3	CH_2 deformation	1425	0
	ν_4	CH_2 wag	1228	−3
	ν_5	D−C−Br deformation	766	3
	ν_6	C−Br stretch	593	2
A″	ν_7	CH_2 antisym. stretch	3045	8
	ν_8	CH_2 twist	1254	−1
	ν_9	CH_2 rock	927	3

[a] From the CCSD(T)/cc-pVTZ anharmonic force field (see text). [b] (obsd − calcd) means observed minus calculated wavenumbers in cm^{-1}.

as a further check for the assignment of the additional bands summarized in Table 3.

The vibrational fundamentals computed with the harmonic CCSD(T)/cc-pVTZ force field and using the x_{ij} constants obtained with the anharmonic force field at the same level of theory are summarized in Table 6, which also reports the description of the normal modes. Due to the general good agreement between calculated and observed values, the molecular force field was employed without introducing any scaling factor.

3.7. The Methylene Stretching Overtone Regions. As illustrated in Table 6 most of the normal modes of CH_2DBr can be described on the basis of the methylene (CH_2) group vibrations. Of particular interest are the symmetric and asymmetric CH_2 stretchings which can also be handled in the local mode approximation as the coupling of two Morse oscillators.[33] Their first overtones, $2\nu_1$ and $2\nu_7$, belong to the same symmetry species A′ and are subjected to Darling−Dennison resonance through the K_{1177} interacting term

$$\langle v_1 + 2, v_7 | \mathbf{H} | v_1, v_7 + 2 \rangle = \frac{K_{1177}}{4}[(v_1 + 1)(v_1 + 2)(v_7 + 1)(v_7 + 2)]^{1/2} \quad (5)$$

where $K_{1177} = x_{17} = -117.6\ cm^{-1}$ in the local mode approximation or $K_{1177} = -126.163\ cm^{-1}$ if calculated employing the cubic and quartic force constants from ab initio calculations.[34] Using the ab initio harmonic wavenumbers, anharmonicity constants, and Darling−Dennison terms, the symmetric resonance matrix (in units of cm^{-1})

	$v_1 = 2$	$v_7 = 2$
$v_1 = 2$	5936	−63
$v_7 = 2$		6025

gives after diagonalization the following eigenvalues: $2\nu_1 = 5904\ cm^{-1}$ and $2\nu_7 = 6058\ cm^{-1}$. These values, once corrected from the errors of the calculated fundamental modes, 8 and 16 cm^{-1} for $2\nu_1$ and $2\nu_7$, respectively, are in excellent agreement with the observed values reported in Table 3.

In the CH_2 stretching second overtone region two different symmetry systems are to be taken into account: (i) $3\nu_1/\nu_1 + 2\nu_7$ of symmetry species A′; (ii) $3\nu_7/2\nu_1 + \nu_7$ of symmetry species A″.

Again the interaction matrix element is related to the Darling−Dennison constant K_{1177} in case (i) and to the $K_{7711} = K_{1177}$ constant in case (ii). The resonance matrix

	$v_i = 3$	$v_i = 1, v_j = 2$
$v_i = 3$	$3\nu_i$	$\frac{\sqrt{3}}{2}K_{iijj}$
$v_i = 1, v_j = 2$		$\nu_i + 2\nu_j$

where $i = 1$ and $j = 7$ for the A′ symmetry block and $i = 7$, $j = 1$ for the A″ symmetry species produce after diagonalization the following values for the three quanta levels: $3\nu_1 = 8710$, $3\nu_7 = 8982$, $2\nu_1 + \nu_7 = 8670$, $\nu_1 + 2\nu_7 = 8928\ cm^{-1}$, all in agreement with the observed wavenumbers (when corrected from the appropriate initial errors between the observed and calculated ν_1 and ν_7 frequencies). The assignment of $3\nu_1$ and $\nu_1 + 2\nu_7$ could be afforded after inspection of the eigenvectors.

Finally, considering the Fermi resonance between the CH_2 symmetric stretching and the overtone of CH_2 deformation, which involves the $2\nu_3/\nu_1$ band system, we have unperturbed values of 2848.8 cm^{-1} ($2\nu_3$) and 2984.6 cm^{-1} (ν_1); removing the offending term from second-order expressions, the corresponding anharmonicity constants become $x_{13}^* = -32.05\ cm^{-1}$ (a similar behavior has been reported in ref 35) and $x_{33}^* = -0.70\ cm^{-1}$. The effective Hamiltonian matrix after diagonalization gives 2832.9 cm^{-1} for $2\nu_3$ and 3000.5 cm^{-1} for ν_1, which are close to those obtained without considering the resonance: 2836.8 and 2996.6 cm^{-1} for $2\nu_3$ and ν_1, respectively. All the computed frequencies are in agreement with the observed ones (see Table 3). On the other hand the anharmonicity constants, x_{13} and x_{33} (see Table 5), for which no Fermi resonance has been accounted, are in good agreement with the experimental values; a closer inspection of the spectra did not give evidence for this kind of interaction.

4. Conclusions

An extensive medium resolution analysis of the infrared absorption bands of CH_2DBr has been performed up to 10000 cm^{-1}. Seventy vibrational states, which account for all the fundamentals and a number of overtones and combinations up to three quantum numbers, have been determined. Eight of the nine fundamentals have been rotationally interpreted. The $v_8 = 1$ level, located at 1252 cm^{-1}, shows a strong Coriolis coupling with the most intense ν_4 band lower in energy by about 27 cm^{-1}. The experimental parameters compared with the calculated values show a satisfactory agreement. The quantum mechanical calculations led to the determination of quadratic, cubic, and quartic force constants from which accurate values of the fundamentals and anharmonicity constants have been obtained. The anharmonicity constants derived from the experimental data show a satisfactory convergence with the calculated values of the anharmonic force field. The results presented in this study add further information useful for the total energy distribution of CH_3Br and should be invaluable to deal with the interpretation of high-resolution spectra of CH_2DBr. With the cubic and quartic force constants of the CCSD(T)/cc-pVTZ anharmonic force field, Darling−Dennison interaction constants could be calculated and employed to clarify the CH_2 stretching first and second overtone spectral regions.

Acknowledgment. The authors gratefully acknowledge the Financial support by PRIN 2007 (project: "*Trasferimenti di energia, carica e molecole in sistemi complessi*") and the High Performance Systems Division of CINECA Supercomputer Centre (Interuniversity Consortium) for the use of computer resources.

References and Notes

(1) Warwick, N. J.; Pyle, J. A.; Shallcross, D. E. *J. Atmos. Chem.* **2006**, *54*, 133–159.

(2) WMO (2007) Scientific Assessment of Ozone Depletion; 2006 Global Ozone Research and Monitoring Project Report No. 50; World Meteorological Organization: Geneva, 2006.

(3) Sinnhuber, B.-M.; Sheode, N.; Sinnhuber, M.; Chipperfield, M. P.; Feng, W. *Atmos. Chem. Phys. Discuss.* **2006**, *6*, 6497–6594.

(4) Jacquemart, D.; Kwabia Tchana, F.; Lacome, N.; Kleiner, I. *J. Quant. Spectrosc. Radiat. Transfer* **2007**, *105*, 264–302.

(5) Tzima, T. D.; Papavasileiou, K. D.; Papayannis, D. K.; Melissas, V. S. *Chem. Phys.* **2006**, *324*, 591–599.

(6) Graner, G. *J. Mol. Spetrosc.* **1981**, *90*, 394–438.

(7) Duncan, J. L. *Spectrochim. Acta, Part A* **1989**, *45A*, 1067–1075.

(8) Law, M. M. *J. Chem. Phys.* **1999**, *111*, 10021–10033.

(9) Schneider, W.; Thiel, W. *J. Chem. Phys.* **1987**, *86*, 923–936.

(10) Schneider, W.; Thiel, W. *Chem. Phys. Lett.* **1989**, *157*, 367–373.

(11) Schneider, W.; Thiel, W. *Chem. Phys.* **1992**, *159*, 49–66.

(12) Venkatraman, R.; Kwiatkowski, J. S.; Bakalarski, G.; Leszczynski, J. *Mol. Phys.* **2000**, *98*, 371–386.

(13) Van Staten, A. J.; Smit, W. M. A. *J. Chem. Phys.* **1977**, *67*, 970–982.

(14) Barrow, G. M.; McKean, D. C. *Proc. R. Soc. London, Ser. A* **1952**, *213*, 27–41.

(15) Dickson, A. D.; Mills, I. M.; Crawford, B. L., Jr. *J. Chem. Phys.* **1957**, *27*, 445–455.

(16) Russel, J. W.; Needham, C. D.; Overend, J. *J. Chem. Phys.* **1966**, *45*, 3383–3398.

(17) Riter, J. R.; Eggers, D. F., Jr. *J. Chem. Phys.* **1966**, *44*, 745–758.

(18) De Hemptinne, M. *Trans. Faraday Soc.* **1946**, *42*, 5–9.

(19) Baldacci, A.; Stoppa, P.; Pietropolli Charmet, A.; Giorgianni, S.; Nivellini, G. *Mol. Phys.* **2005**, *103*, 2803–2811.

(20) Raghavachari, K.; Trucks, G. W.; Pople, J. A.; Head-Gordon, M. *Chem. Phys. Lett.* **1989**, *157*, 479–483.

(21) Császár, A. G. *The Encyclopedia of Computational Chemistry*; Schleyer, P. v. R., Allinger, N. L., Clark, T., Gasteiger, J., Kollman, P. A., Schaefer, H. F., III, Schreiner, P. R., Eds.; Wiley: Chichester, 1998; pp 13−30.

(22) Dunning, T. H., Jr. *J. Chem. Phys.* **1989**, *90*, 1007–1023.

(23) Wilson, A. K.; Woon, D. E.; Peterson, K. A.; Dunning, T. H., Jr. *J. Chem. Phys.* **1999**, *110*, 7667–7676.

(24) Stanton, J. F.; Lopreore, C.; Gauss, J. *J. Chem. Phys.* **1998**, *108*, 7190–7196.

(25) Stanton, J. F.; Gauss, J.; Watts, J. D. ; Szalay, P. G.; Bartlett, R. J. with contributions from Auer, A. A.; Bernholdt, D. E.; Christiansen, O.; Harding, M. E.; Heckert, M.; Heun, O.; Huber, C.; Jonsson, D.; Jusélius, J.; Lauderdale, W. J.; Metzroth, T.; Michauk, C.; O'Neill, D. P.; Price, D. R.; Ruud, K.; Schiffmann, F.; Varner, M. E.; Vázquez, J. and the integral packages MOLECULE (Almlöf, J.; Taylor, P. R.), PROPS (Taylor, P. R.), and ABACUS (Helgaker, T.; Jensen, H. J. Aa.; Jørgensen, P.; Olsen, J.). For the current version, see http://www.aces2.de.

(26) Purvis, G. D., III; Bartlett, R. J. *J. Chem. Phys.* **1982**, *76*, 1910–1918.

(27) Helgaker, T.; Jørgensen, P.; Olsen, J. *Molecular Electronic-Structure Theory*; J. Wiley: Chichester, 2000; Chapter 15.

(28) Helgaker, T.; Gauss, J.; Jørgensen, P.; Olsen, J. *J. Chem. Phys.* **1997**, *106*, 6430–6440.

(29) Aldous, J.; Mills, I. M. *Spectrochim. Acta* **1962**, *18*, 1073–1091.

(30) Allen, W. D.; Császár, A. G.; Horner, D. A. *J. Am. Chem. Soc.* **1992**, *114*, 6834–6849.

(31) Mills, I. M. *Molecular Spectroscopy: Modern Research*; Narahari, Rao K., Mathews, C. W., Eds.; Academic Press: New York, 1972; Vol. 1, pp 115−140.

(32) Papoušek, D.; Aliev, M. R. *Molecular Vibrational-Rotational Spectra*, Elsevier: Amsterdam, 1982; p 160.

(33) Mills, I. M.; Robiette, A. G. *Mol. Phys.* **1985**, *56*, 743–765.

(34) Lehmann, K. K. *Mol. Phys.* **1989**, *66*, 1129–1137, erratum **1992**, *75*, 739.

(35) McKean, D. C.; Craig, N. C.; Law, M. M. *J. Phys. Chem. A* **2008**, *112*, 10006–10016.

JP901577X